ARTICLE OPEN

Check for updates

Diverging asymmetry of intrinsic functional organization in autism

Bin Wan[1,2,3,4]✉, Seok-Jun Hong[5], Richard A. I. Bethlehem[6], Dorothea L. Floris[7,8], Boris C. Bernhardt[9] and Sofie L. Valk[1,4,10]✉

Autism is a neurodevelopmental condition involving atypical sensory-perceptual functions together with language and socio-cognitive deficits. Previous work has reported subtle alterations in the asymmetry of brain structure and reduced laterality of functional activation in individuals with autism relative to non-autistic individuals (NAI). However, whether functional asymmetries show altered intrinsic systematic organization in autism remains unclear. Here, we examined inter- and intra-hemispheric asymmetry of intrinsic functional gradients capturing connectome organization along three axes, stretching between sensory-default, somatomotor-visual, and default-multiple demand networks, to study system-level hemispheric imbalances in autism. We observed decreased leftward functional asymmetry of language network organization in individuals with autism, relative to NAI. Whereas language network asymmetry varied across age groups in NAI, this was not the case in autism, suggesting atypical functional laterality in autism may result from altered developmental trajectories. Finally, we observed that intra- but not inter-hemispheric features were predictive of the severity of autistic traits. Our findings illustrate how regional and patterned functional lateralization is altered in autism at the system level. Such differences may be rooted in atypical developmental trajectories of functional organization asymmetry in autism.

Molecular Psychiatry; https://doi.org/10.1038/s41380-023-02220-x

INTRODUCTION

Autism is a heterogeneous neurodevelopmental condition with a prevalence exceeding 2% in a recent survey in the U.S. [1]. It is characterized by life-long differences in social interaction and communication alongside restricted and repetitive interests/behaviors [2]. The widespread behavioral differences observed in individuals with autism are paralleled by reports of structural and functional alterations in both sensory and association regions of the brain [3–12].

Whole brain differences in structure and function between autistic and non-autistic individuals (NAI) are augmented by observations of disrupted patterns of brain asymmetry [13, 14], possibly linked to abnormal lateralization of functional processes supporting language and social cognition [15–20]. Asymmetry is a key feature of brain organization, supporting a flexible interplay between specific local neural modules linked to functional specialization underlying human cognition [21]. In particular, left-hemispheric regions have been reported to be biased to interact more strongly within the hemisphere, whereas interactions of the right hemispheric regions are more bilateral [22]. Recent work has shown that individuals with autism display marked and widespread atypical patterns of asymmetry of local structure [13]. Such differences may reflect changes in network-level embedding, in particular in association regions, as measured by structural covariance [14]. Functionally, individuals with autism exhibit idiosyncratic alterations in homotopic inter-hemispheric connectivity patterns, indicating more variation in the autistic population [23, 24]. Further, they show atypical rightward functional lateralization in mean motor circuit connectivity [25]. Independent component analysis (ICA) using the resting state functional connectome suggests that component loadings are more rightward in individuals with autism [26]. Last, decreased asymmetry of functional activation patterning has been observed in individuals with autism during the letter fluency task [27]. Functional differences may be rooted in altered developmental trajectories of functional lateralization in autism [28], leading to altered global features of brain organization and asymmetry, as captured by low dimensional connectome embeddings [29, 30]. Thus, observed localized asymmetry differences may reflect altered system-wide functional organization.

To further understand system-level functional lateralization alterations in autism, here we investigated the asymmetry of intra- and inter-hemispheric functional connectome gradients [22, 31], which robustly capture associated organizational features [30, 32].

[1]Otto Hahn Research Group Cognitive Neurogenetics, Max Planck Institute for Human Cognitive and Brain Sciences, Leipzig, Germany. [2]International Max Planck Research School on Neuroscience of Communication: Function, Structure, and Plasticity (IMPRS NeuroCom), Leipzig, Germany. [3]Department of Cognitive Neurology, University Hospital Leipzig and Faculty of Medicine, University of Leipzig, Leipzig, Germany. [4]Institute of Neuroscience and Medicine (INM-7: Brain and Behaviour), Research Centre Jülich, Jülich, Germany. [5]Centre for Neuroscience Imaging Research, Institute for Basic Science, Department of Global Biomedical Engineering, Sungkyunkwan University, Suwon, South Korea. [6]Department of Psychology, University of Cambridge, Cambridge, UK. [7]Department of Psychology, University of Zürich, Zürich, Switzerland. [8]Department of Cognitive Neuroscience, Donders Institute for Brain, Cognition and Behaviour, Radboud University Nijmegen Medical Centre, Nijmegen, Netherlands. [9]McConnell Brain Imaging Centre, Montréal Neurological Institute and Hospital, McGill University, Montréal, QC, Canada. [10]Institute of Systems Neuroscience, Heinrich Heine University Düsseldorf, Düsseldorf, Germany. ✉email: binwan@cbs.mpg.de; valk@cbs.mpg.de

Received: 6 April 2023 Revised: 1 August 2023 Accepted: 4 August 2023
Published online: 16 August 2023

Cortical regions show organizational axes reflecting integration and segregation [22] along different dimensions [32–35]. The principal gradient (G1) transitions between sensory and default mode networks, the secondary gradient (G2) between sensory and visual cortices, and the tertiary gradient (G3) between default mode and multiple demand networks. These gradients can be reliably identified [29], and are among the most widely studied in the gradient literature [36]. Together, these gradients describe patterns of developmental and heritable variation in the human cortex [37–39]. In previous work, we and others [31, 40, 41] have shown that, whereas intrinsic functional organization within left and right hemispheres differentiates sensory (visual, sensory-motor) from transmodal (e.g., DMN, control, language) networks, there are also subtle asymmetries. For example, regions involved in language processing show stronger differentiation from sensory anchors in the left hemisphere, whereas regions associated with executive function show stronger differentiation from sensory anchors in the right hemisphere. Given that language impairments and verbal imbalances are key traits of autism [42–45] and executive function may underlie the psychological and behavioral neurodivergence observed in autism [46, 47], we hypothesize that atypical lateralization axes in autism may contribute to autistic behaviors.

To answer our research question, we first compared the asymmetry of functional gradients between autistic individuals and NAI to reveal the differences between groups. Because brain asymmetry [48, 49] and gradients [37, 39, 50] are affected by age, we also evaluated the interaction of age and autism status to reveal the cross-sectional developmental trajectory. Given the heritability of functional gradient asymmetry [31], and of autism [51, 52], we used prior heritability estimates [31], to evaluate whether autism is associated with differences in regions found to be heritable in adulthood. Finally, supervised machine learning was used to establish phenotypical relevance. We also tested robustness using the functional connectome after global signal regression (GSR).

RESULTS

Data demographics

We utilized resting-state fMRI data from five sites from the Autism Brain Imaging Data Exchange (ABIDE-I) [53] including: New York University Langone Medical Center (NYU-I, $n = 86$), University of Pittsburgh, School of Medicine (Pitt, $n = 39$), and University of Utah, School of Medicine (USM, $n = 83$), as well as Trinity Center for Health Sciences, Trinity College Dublin (TCD, $n = 32$) and NYU-II ($n = 43$) from ABIDE-II [54]. We selected those sites that included children, adolescents, and adults. All participants were male ($n_{\text{autism}} = 140$ and $n_{\text{NTC}} = 143$) with age ranging from 5 to 40 years. There was no significant age difference ($t = -0.030$, $p = 0.976$) or simple size across data sites ($t = 5.212$, $p = 0.266$) between individuals with autism and NAI. The resting state fMRI data were preprocessed based on C-PAC (https://fcp-indi.github.io/). Functional connectome gradients of each individual were aligned to the group-level gradient template that is derived from Human Connectome Project (HCP) [31]: sensory-default (G1), somatomotor-visual (G2), and default-multiple demand (G3) gradients. Procrustes is a technique for rotating a matrix to maximum similarity with a target matrix minimizing sum of squared differences. The inclusion and exclusion criteria and detailed computation can be seen in the *Methods*.

The full intelligence quotient (FIQ) and Autism Diagnostic Observation Schedule (ADOS, Generic version) score are shown in Supplementary Table S1. Of note, there are differences between autism and NAI in FIQ ($t = -5.710$, $p < 0.001$) and head motion ($t = 2.636$, $p = 0.009$). Multi-site effect was removed before analyses via data harmonization that follows an empirical Bayesian approach to balance the effects of each scanner/batch [55].

Asymmetry along functional organization axes (Fig. 1)

We first computed the functional connectome for each individual, and applied diffusion embedding [30, 32] to decompose the first 10 gradients of different connectivity patterns (i.e., LL connectome: from left to left, LR connectome: from left to right, RL connectome: from right to left, and RR connectome: from right to right). Then, we aligned individual gradients of all the participants to the HCP group-level gradient of the left-left functional connectivity pattern [31] with Procrustes rotations. This allowed direct comparison of the organization of functional asymmetry across groups and individuals, in line with previous work [4, 9, 10, 31]. Individual functional gradient computation and analyses with Python packages BrainSpace [30] and BrainStat [56] are described in the *Methods*.

Next, we calculated the asymmetry index (AI) along the three organizational axes (Fig. 1A) for intra-hemispheric FC patterns (LL minus RR) and inter-hemispheric FC patterns (LR minus RL) following previous work [31]. Overall, the spatial asymmetric pattern was similar to the HCP asymmetric pattern [31], with NAI showing more similar patterns than autism (Supplementary Results). We then took a multivariate approach using Hotelling's T to discover shared effects across the three eigenvectors. In post-hoc analyses we further investigated contributions of individual gradients to the overall effects, correcting for the number of gradients considered ($p < 0.05/3$). For this analysis, age effect was entered as a covariate during data harmonization.

Parcel-wise multivariate analyses with $p_{\text{FDR}} < 0.05$ mapped overall differences between individuals with autism and NAI (Fig. 1B). This revealed group differences in language-related and somatosensory areas for intra-hemispheric patterns, and inter-hemispheric differences in dorsal prefrontal, superior temporal, and postcentral cortices. We performed post-hoc single gradient comparisons of these parcels (Supplementary Results and Table S2). Positive and negative t-values indicate lower and higher left-right asymmetry in individuals with autism relative to NAI. In particular, for intra-hemispheric G1, parcels included medial posterior superior frontal lobule (SFL, $t = 2.758$, $p = 0.006$), area 43 (posterior opercular, $t = -3.058$, $p = 0.002$), and the dorsal posterior superior temporal sulcus (STSdp, $t = 3.796$, $p < 0.001$). For inter-hemispheric G1 parcels included area 33pr (anterior cingulate, $t = -2.436$, $p = 0.015$), area a24pr (anterior cingulate, $t = -4.390$, $p < 0.001$), area p32pr (anterior cingulate, $t = -3.548$, $p < 0.001$), area 47m (frontal pole, $t = 2.648$, $p = 0.009$), area 47s (frontal pole, $t = 3.384$, $p < 0.001$), auditory 5 complex (A5, $t = 2.813$, $p = 0.005$), dorsal anterior superior temporal sulcus (STSda, $t = 3.838$, $p < 0.001$), and temporo-parieto-occipital junction 1 (TPOJ1, $t = 2.815$, $p = 0.005$). The parcel labels refer to ref. [57]. G2 and G3 showed less strong asymmetric differences between individuals with autism and NAI and have been described in the Supplementary Results.

When evaluating network-wise asymmetries [58], we observed four significant networks for multivariate comparisons after FDR correction (Fig. 1B and Supplementary Table S3). Only three were observed with statistical significance in single-gradient analyses (Fig. 1C and Supplementary Table S3). Specifically, the language network (Lan., intra-hemispheric G1, $t = 3.682$, $p < 0.001$; inter-hemispheric G1, $t = 3.973$, $p < 0.001$), cingulo-opercular network (CON, inter-hemispheric G1, $t = -2.248$, $p = 0.007$), and somatomotor network (SMN, inter-hemispheric G3, $t = 3.443$, $p < 0.001$) showed differentiable asymmetry. Results remained robust when performing GSR. Detailed reports can be found in Supplementary Results Fig. S2. Findings did not change after including FIQ and head motion as covariates during data harmonization.

Inter-subject similarity analyses across each data site [24] tested the populational differences between individuals with autism and NAI in cortical functional asymmetric patterns. We observed that individuals with autism showed a lower similarity score relative to NAI along the three axes. Detailed reports are shown

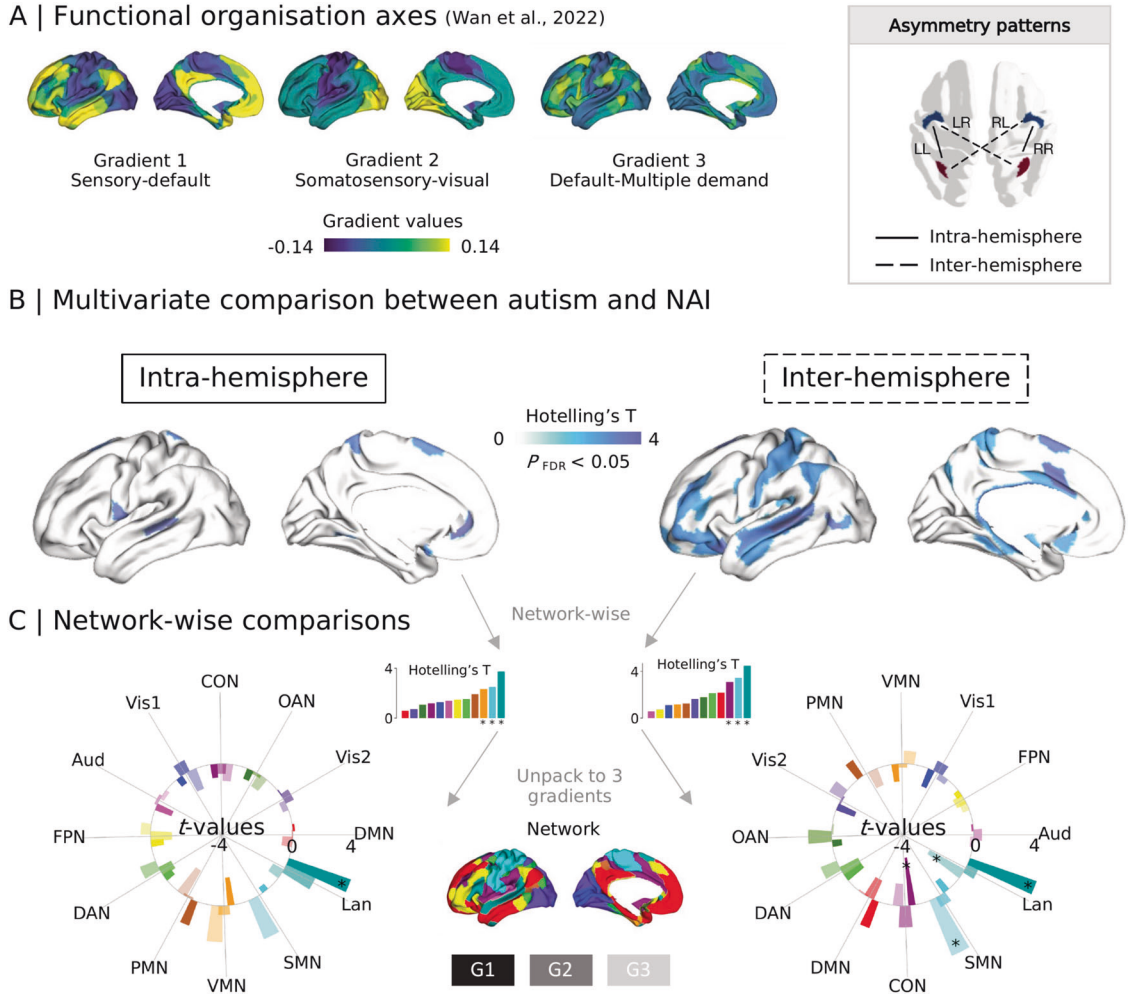

Fig. 1 Comparison between individuals with autism and NAI in gradient asymmetry index along functional organizational axes. A HCP group-level gradients of left-left (LL) functional connectome described by [31] including G1: sensory-default gradient, G2: somatosensory-visual gradient, and G3: default-multiple demand gradient. Asymmetry has intra- and inter-hemispheric patterns derived from [LL, RR] and [LR, RL] functional connectome. **B** Multivariate comparison across G1, G2, and G3. The brain maps show the Hotelling's *T* values ($p_{FDR} < 0.05$) for multivariate comparison. **C** Network-wise comparisons. The multivariate analyses were summarized from parcel-wise comparison using multi-modal parcellation [57] to network-wise comparison using Cole-Anticevic (CA) atlas [58]. Radar-bar plots show network-wise decomposition results (from multivariate to single gradient). Dark, middle dark, and light colors indicate *t*-values of each network along G1, G2, and G3. *marks significant networks. NAI non-autistic individuals, Vis1: primary visual network, Vis2: secondary visual network, SMN: somatomotor network, CON cingulo-opercular network, DAN dorsal attention network, Lan. language network, FPN frontoparietal network, Aud. auditory network, DMN default mode network, PMN posterior multimodal network, VMN ventral multimodal network, OAN orbito-affective network.

in Supplementary Results and Supplementary Table S8. This suggests that autism is quite heterogeneous in terms of functional organization asymmetry.

Developmental effects (Fig. 2)

To explore whether the asymmetry of functional gradients develops differently between individuals with autism and NAI, we categorized participants into three age groups including children (5–12 years, $n = 74$), adolescents (12–18 years, $n = 93$), and adults (18–40 years, $n = 130$).

We first examined whether there were age differences within autism and NAI groups. In the comparisons between age groups, we set $p < 0.05/3$ (Bonferroni correction) as the significance level. We observed no significant asymmetry changes with age in autism. However, there were significant age differences in Vis1, Lan., and OAN in NAI. For example, in NAI, children showed increased leftward asymmetry relative to adults in Lan. along G3 (intra-hemispheric, $t = -3.852$, $p < 0.001$; inter-hemispheric, $t = -2.443$, $p = 0.016$). See Supplementary Results and Supplementary Table S4 for further details. We then studied the interaction between age and autism status to evaluate whether the age effects are different between autism and NAI. Parcel-wise multivariate analyses revealed interaction effects of age with autism status in parcels primarily located in dorsolateral prefrontal and posterior temporal cortices for the intra-hemispheric pattern, and in parcels mainly located in postcentral and visual cortices for the inter-hemispheric pattern (Fig. 2A). The detailed parcel-wise and single-gradient results are presented in Supplementary Table S5. Regarding network-wise comparisons, Fig. 2B illustrates intra- and inter-hemispheric patterns of age by autism status effects (Supplementary Table S5). Among them, we found interaction effects in Lan. along intra-hemispheric G3 ($t = 3.830$, $p < 0.001$) after Bonferroni correction. Interaction between autism status and age using GSR replicated the intra-hemispheric asymmetry results but not the inter-hemispheric asymmetry results (Supplementary Results). Results did not change after including FIQ and head motion as covariates during data harmonization.

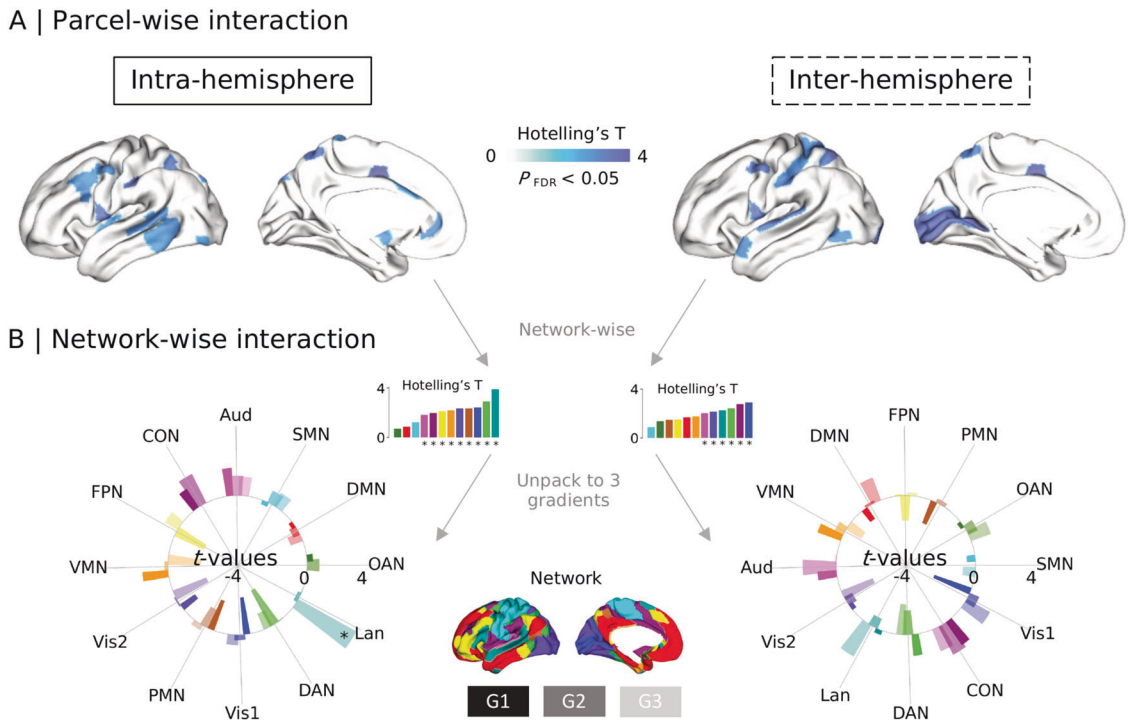

Fig. 2 Interaction effects between age and autism status on asymmetry index (AI). A Parcel-wise interaction using multivariate analyses. The brain maps show the Hotelling's *T* values ($p_{FDR} < 0.05$) for multivariate comparison across the three gradients. **B** Network-wise interaction from multivariate to single gradient. Vis1: primary visual network, Vis2: secondary visual network, SMN somatomotor network, CON cingulo-opercular network, DAN dorsal attention network, Lan. language network, FPN frontoparietal network, Aud. auditory network, DMN default mode network, PMN posterior multimodal network, VMN ventral multimodal network, OAN orbito-affective network.

Analyses for diagnostic differences in each age group have been shown in Supplementary Results and Supplementary Table S6. Overall, diagnostic differences in Lan. along G1 and SMN along G3 were present in adolescents but not in children or adults.

Meta-analytic functional decoding and heritability (Fig. 3)

Having established marked alterations in asymmetry of functional organization between individuals with autism and NAI, which varied across age-groups, we further aimed to contextualize the findings. In particular, to explore how the differences between autism and NAI are related to cognitive functions, we performed meta-analytic decoding using NeuroSynth [59] using 24 terms-related z-activation maps, similar to previous work [31, 32, 38]. Second, we performed decoding of asymmetry effects relative to heritability of asymmetry observed in previous work, based on HCP twin-based data (Fig. 3A) from [31]. Details can be found in the *Methods*.

Regarding functional decoding, the *t*-map calculated from Fig. 3B of intra-hemispheric G1 (Fig. 3C) showed strong relevance to language, reading, and social cognition (Fig. 3D). The *t*-map of inter-hemispheric G1 showed strong relevance to auditory, language, and social cognition. Autism status*age effects along intra-hemispheric G3 showed strong relevance to auditory, language, and affective. Autism status*age effects along inter-hemispheric G3 showed strong relevance to affective, auditory, and autobiographical memory. Other functional decoding results are shown in Supplementary Results.

Heritability is a marker that illustrates the proportion of variance across a population to be attributed to genetic factors. Here we sought to understand whether regions showing asymmetry differences between individuals with autism and NAI would be heritable within a population in young adulthood (22–37 years, HCP sample), as a proxy for a potential genetic versus environmental interplay associated with asymmetry. We extracted heritability values with standard error (SE) of the regions displaying diagnostic effects (Fig. 3E and Supplementary Table S7). The regions displaying diagnostic effects along intra-hemispheric G1 showed low heritability, ranging from 0.069 to 0.083. The regions displaying diagnostic effects along inter-hemispheric G1 showed moderate heritability, ranging from 0.074 to 0.293, of which 33pr ($h^2 = 0.163$, SE = 0.057, $p_{FDR} = 0.006$), 47 m ($h^2 = 0.137$, SE = 0.062, $p_{FDR} = 0.027$), A5 ($h^2 = 0.162$, SE = 0.065, $p_{FDR} = 0.015$), STSdp ($h^2 = 0.146$, SE = 0.062, $p_{FDR} = 0.020$), and TPOJ1 ($h^2 = 0.293$, SE = 0.061, $p_{FDR} < 0.001$) survived after FDR correction. Moreover, STSda ($h^2 = 0.133$, SE = 0.059, $p_{FDR} = 0.038$) along inter-hemispheric G2, SFL ($h^2 = 0.212$, SE = 0.060, $p_{FDR} = 0.001$), 47l ($h^2 = 0.267$, SE = 0.065, $p_{FDR} < 0.001$), and FST ($h^2 = 0.133$, SE = 0.062, $p_{FDR} = 0.028$) along inter-hemispheric G3 survived after FDR correction.

Phenotypic associations (Fig. 4)

Lastly, we aimed to test whether asymmetry features (540 features based on 180 parcels * 3 gradients) can predict autistic traits as measured by ADOS ($n = 132$). To do so, we combined a linear regression with elastic net 5-fold cross validation (CV) with a supervised machine learning approach (Fig. 4A) using scikit-learn (https://scikit-learn.org). Here we used L1_ratio = 0.1 to set up the regularization. Details using other L1_ratio parameters can be found in Supplementary Results.

Briefly, we randomized the whole sample for train-test (4:1) samples for 100 permutations. Multi-site and age effects were regressed out using neuroCombat data harmonization [55] for training and testing samples separately. To automatically tune hyperparameters, we set a series of alphas from 0.0001 to 1. Elastic net with 5-fold CV estimated the models. The model with the lowest mean absolute error (MAE) was selected as being well-trained. Finally, to evaluate how much the model fit the testing sample, we calculated the Pearson *r* between the actual score and

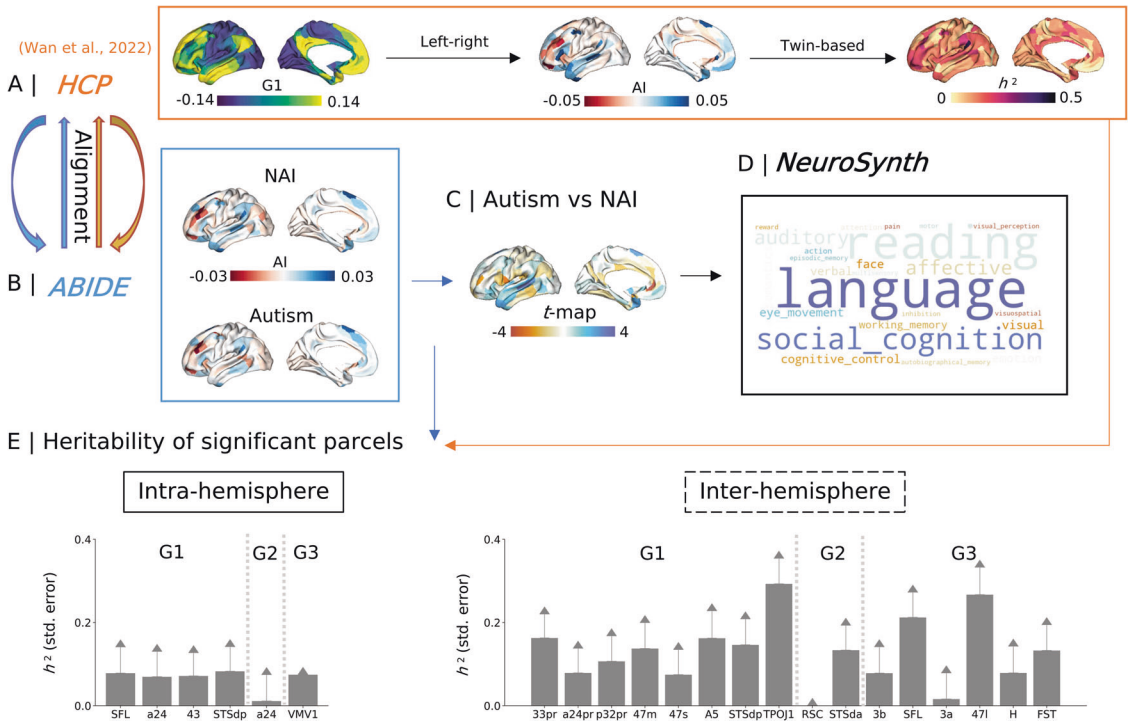

Fig. 3 Heritability and meta-analytic decoding for *t*-map (G1). A Yellow square shows how the heritability was computed by [31] using HCP twin-based data. Details can be seen in *Methods*. **B** Blue square is the asymmetry in autism and NAI using the same pipeline to align individual gradients to the HCP template. **C** Comparison between autism and NAI in asymmetry brain map. We showed the *t*-map here for functional decoding. **D** Black square describes functional decoding of meta-analytic maps using NeuroSynth [59]. The bigger size of the text indicates the larger relevance to higher absolute *t*-values. The details regarding how to generate the maps and word clouds can be seen in the *Methods*. We also performed functional decoding for the other asymmetry maps (Supplementary Results). **E** Illustrates the heritability with standard error estimates derived from panel **A**.

the predicted score in the testing sample. Across 100 permutations, MAE distributions are shown in Fig. 4B with the mean ± SD being 4.875 ± 0.508 for the training sample and 4.314 ± 0.595 for the testing sample.

Figure 4C illustrates the frequency of each selected feature across the 100 permutations. In our pipeline, each feature had at least 50% possibility of being selected. High frequency occurred in DMN, PFN, and Lan. along G1, DAN, Lan., and OAN along G2, and Lan., FPN, and VMN along G3. Out-of-sample prediction suggests mean ± SD Pearson *r* to be 0.215 ± 0.148 for ADOS total score (Fig. 4D). However, the models using inter-hemispheric asymmetry features did not show good performance, with a mean ± SD Pearson *r* of −0.035 ± 0.108 for ADOS total score (Supplementary Results). Regarding prediction for ADOS subscores, intra-hemispheric asymmetry features fit positively for communication (Pearson $r = 0.130 \pm 0.142$) and social (Pearson $r = 0.153 \pm 0.160$) but not RRB (Pearson $r = -0.097 \pm 0.121$), possibly in line with functional relevance of functional brain asymmetry.

DISCUSSION

In the current work, we studied the difference in asymmetry of functional organization between autistic and NAI. Here functional organization was defined within a gradient framework [30, 32, 36], differentiating three main axes of organization differentiating: sensory from default networks, linked to a differentiation of perceptual from abstract cognitive functions (G1), sensorimotor from visual networks (G2), and default from multiple demand networks, associated with a differentiation of attention/control functions from more task-negative functions such as autobiographical memory (G3) [32, 33, 60–62]. Overall we observed that asymmetry effects could be best described by a combination of asymmetry in these axes; yet, we observed axis-specific effects as well. For example, the language network showed an altered embedding along the sensory-transmodal intrinsic functional axes when comparing neurotypical controls and autistic individuals. On the other hand, when studying age-related change in embedding, we found that again the language network showed altered embedding, however, this time, this was largely linked to its embedding on a functional axis differentiating attention/control from the off-task, mnemonic functions, G3. Moreover, individuals with autism showed higher population heterogeneity for the spatial patterns of asymmetry. Intra-hemispheric asymmetry in language areas such as STS, found to differ between autistic individuals and NAI, were previously found to have low heritability in a young adult sample of NAI. However, group differences in inter-hemispheric asymmetry were observed to have moderate heritability strengths in NAI. These diverging patterns also suggest that both genetic and environmental components may be important to consider in the context of functional asymmetry differences between autism and NAI across development. Last, we found that, rather than inter-hemispheric asymmetry features, intra-hemispheric asymmetry features were more predictive of autistic traits. Together, our work shows extended differences in functional organization asymmetry between autism and NAI, which may be rooted in development and highly variable across individuals.

In the current work we leveraged the ABIDE sample, an openly available, multi-site cohort of individuals with autism and NAI [53, 54] through data harmonization. Previous work on the same sample has revealed that both sensory and default regions are functionally more integrated in autism relative to NAI [4]. Here, we extend these findings by showing that the language network had higher integration in the left hemisphere in NAI whereas in autism

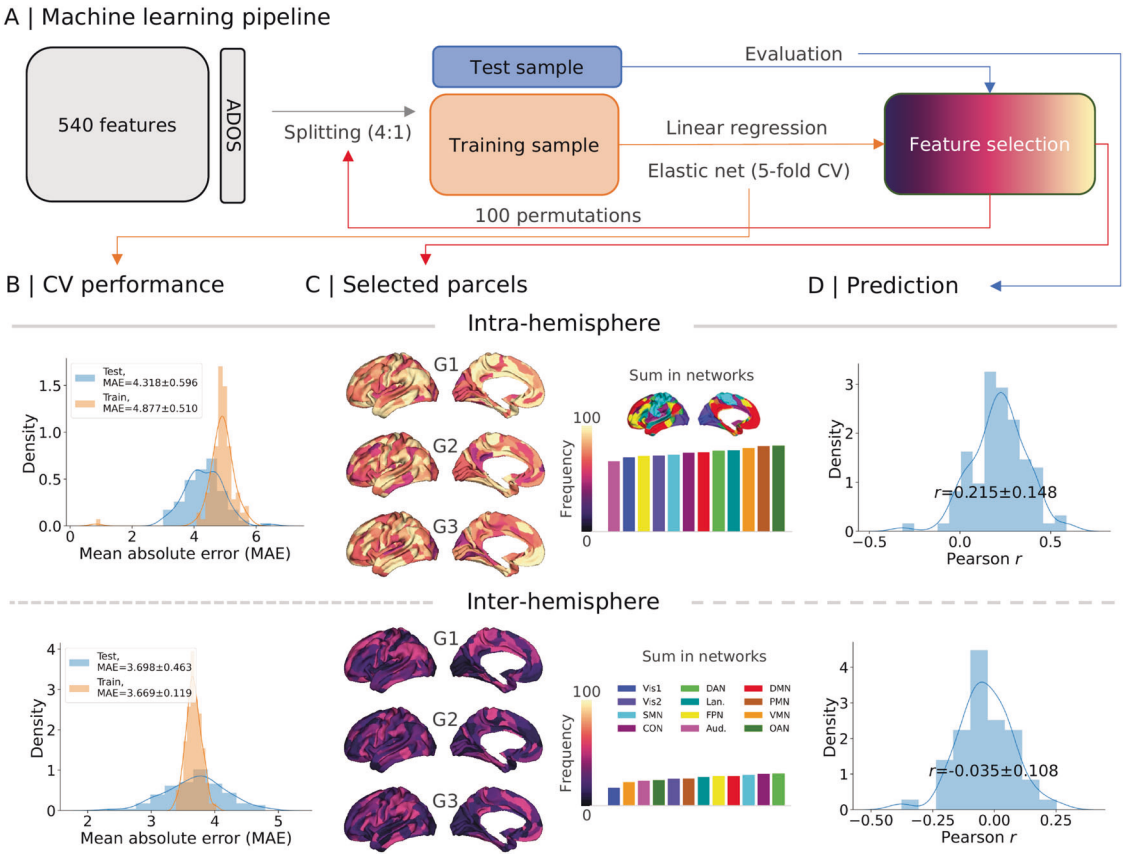

Fig. 4 Autism traits and functional asymmetry. A Machine learning pipeline. We used 540 features (180 parcels * 3 gradients) to predict the total score of ADOS. All subjects were split into 4:1 training:test samples. Linear regression with elastic net (L1_ratio = 0.1) was the feature selector during which 5-fold cross validation was employed. We permuted this procedure 100 times by splitting the subjects randomly. **B** Shows how the model works in the training and testing samples using mean absolute error (MAE) during the 100 permutations. **C** Summarizes the frequency of this feature being selected across the 100 permutations. **D** Illustrates the distribution of correlations between the observed ADOS total score and predicted ADOS total score in the testing samples across the 100 permutations. Vis1: primary visual network, Vis2: secondary visual network, SMN somatomotor network, CON cingulo-opercular network, DAN dorsal attention network, Lan. language network, FPN frontoparietal network, Aud. auditory network, DMN default mode network, PMN posterior multimodal network, VMN ventral multimodal network, OAN orbito-affective network.

higher integration was found in the right hemisphere. Interestingly, networks that show rightward asymmetry in healthy individuals, e.g., FPN and CON along the sensory-default axis [31], are more rightward in individuals with autism compared with NAI. This differing processing pattern between hemispheres in autism is consistent with the idea of pervasive rightward lateralization in the disorder [25, 26, 63]. Cardinale and colleagues (2013) used ICA to reveal 10/17 asymmetric networks and found that these networks (visual, auditory, motor, executive, language, and attentional) without exception display atypical rightward asymmetry in autism. Atypical motor performance in autism is correlated with their rightward motor circuits [25]. These findings are mirrored by task-based reports, including language [27, 64] and face processing [65] tasks and may be linked to increased rightward or decreased leftward functional activation in autism [27]. As a system-level measurement, the gradients approach describes a regional feature as a function of an interregional embedding [36]. Thus, observed local regional asymmetries reported in prior work may result from systemic alterations in integration and segregation of functional connectivity as reported here.

Both cortical asymmetry and organization of intrinsic function show developmental change. For example, though left-right asymmetry is observed in the neonatal brain, frontal and temporal asymmetry in neonates differs from observations in adults [66]. Here, we revealed a developmental component to deviating asymmetry of functional organization in language-related regions. Such a developmental alteration may be in line with reported delays in language and communication in autism [67]. The developmental trajectory of language-task activation lateralization follows an upwards trend from early childhood to adolescence, plateaus between 20 and 25 years, and slowly decreases between 25 and 70 years [68]. This converges with our observations in language network asymmetry using a system-level approach along G1, i.e., increased leftward asymmetry from childhood to adolescence and slightly decreased asymmetry from adolescence to adulthood in NAI. At the same time, we did not observe such developmental changes in autism, nor an interaction between autism status and age. This may indicate that the embedding of the language network, relative to attention networks, shows differential changes during development in individuals with autism relative to NAI, whereas its embedding between perceptual and abstract cognitive functions varies within autism, relative to NAI, irrespective of age. It has been suggested that initially bilateral language activation becomes more left-lateralized in typically developing children, whereas children with autism show a different developmental trajectory becoming increasingly rightward lateralized [28]. This indicates there should be an interaction with respect to language network asymmetry. We indeed observed such an interaction along G3. Language network asymmetry along G3 alters its direction from leftward to rightward during typical maturation whereas for autism we observed a subtle and leftward trend. It may suggest that language functions

have multidimensional maturation trajectories (i.e., G1 and G3). The network-wise results were driven by language-related parcels in the temporal gyrus instead of frontal gyrus. It is of note that the current sample includes largely high-functioning individuals with autism. Yet, oral language impairments are observed in various degrees along the autism spectrum [67] and language comprehension (especially under social context), instead of oral language, might be more apparent in individuals with high-functioning autism. Thus, in future work it will be relevant to study asymmetry in brain organization in a possibly more heterogeneous sample of individuals with autism.

Importantly, we observed age differences in functional gradient asymmetry in NAI but not in autism. This suggests that whilst asymmetry of functional organization in NAI changes over the course of development, this is not the case in individuals with autism. Other work also supports the notion that age effects of brain asymmetry are not found in individuals with autism [48, 68–70]. This may reflect a maturation failure model in neurodevelopmental conditions and disorders [71], which in the case of autism may lead to different asymmetry development. Research shows that cortical asymmetries may largely be determined prenatally and that they may constrain the development of lateralized functions in later life [66]. This suggests asymmetry is determined by genetics and environment in utero. In particular, environmental effects over the left hemisphere may be stronger than the right hemisphere in utero [72]. Thus, the maturation alterations of brain asymmetry in autism might result from a complex interplay between genetic and environmental effects. Our study analyzed cross-sectional development, yet longitudinal data are necessary to evaluate the maturation failure model in autism.

Further investigating the interplay of developmental effects from genes on brain asymmetry, we evaluated whether regions showing differential asymmetry in autism are heritable in a normative non-autistic adult sample [31]. We found that temporal language regions such as posterior STS and TPOJ1 along G1 between autism and NAI were heritable, whereas they were not heritable under intra-hemispheric connections. This different heritability of asymmetry patterns may suggest that the global feature in superior STS is more variable during intra-hemispheric specialization and may show stronger genetic constraints during inter-hemispheric specialization. Recent work using single-nucleotide polymorphisms (SNPs)-based analyses in the UK Biobank suggest high heritability in surface area asymmetry in these two regions. Further work, using more refined genetic imaging analysis, may help to further understand the neurobiological mechanisms underlying regional asymmetry and its functional consequences [73]. Thus, inter- but not intra-hemispheric connectivity might be linked in some manner to additive genetic factors. As mentioned previously, environmental factors may have double effects on the left vs right hemisphere in brain volume in utero development [72]. One possibility is that genes influence spatial organization in the right hemisphere, relevant to the inter-hemispheric function of superior STS, but that genes associated with autism impact inter-hemispheric connectivity. Further work using multilevel genetic and imaging data as well as brain models may help provide answers to these questions.

Lastly, we identified multiple areas related to autism traits via machine learning procedures similar to previous work [4, 9]. This indicates that the model optimizes the parameters by averaging the features' effects in autism and may reflect the complexity of autism traits using asymmetry features. We observed that the prediction using inter-hemispheric features is not as good as using intra-hemispheric features to predict ADOS total score. Follow-up indicated that subscores of communication and social traits showed acceptable out of sample prediction. Yet, repeated behaviors did not, underscoring the social and communicative trait relevance of individual variation in functional asymmetry. The differentiation between intra- and inter-hemispheric differences in terms of their predictability may again point to differential association between developmental and baseline effects. Indeed, intra- and inter-hemispheric asymmetry is primarily differentiated by the developmental timing of the role of corpus callosum [74, 75]. Some studies have reported atypical cross-hemispheric connectivity and reduced corpus callosum size in autism compared to NTC [76, 77]. However, agenesis of the corpus callosum is not enough to specify the autistic traits [78]. Future work may investigate the interplay between genes and environment in the context of intra- and inter-hemispheric connectivity and its clinical relevance to autism. Such differences may have already led to the differential idiosyncrasy of inter- and intra-hemispheric patterning, with idiosyncrasy of inter-hemispheric connectivity to be more extended in autism.

Overall, through studying the organization of intrinsic functional asymmetry, our work provides a framework to study hemispheric differences in individuals with autism versus NAI. However, there are several limitations to note. First of all, the current study was based on neuroimaging data from multiple acquisition sites, enhancing the sample size but at the same time also introducing potential site-related confounds. We used data harmonization [55] to reduce this influence as much as possible. Second, the enrichment decoding results are indirect. If we want to understand the genetic basis and cognitive relevance of asymmetry in autism and healthy individuals, it is necessary to measure genetic and cognitive features in autism. Moreover, in the current sample, we could not provide the causal link between development and functional asymmetry. Longitudinal design and/or high-risk autism models may help to highlight the neurodevelopmental foundations of functional asymmetry in autism and guide implications for support. Finally, we excluded autistic females, however, research shows that brain lateralization differs by sex [41, 48, 79, 80] and autism shows sex and gender differences in prevalence, behavior and brain [1, 81–84]. Future studies should investigate whether there exist sex and gender-differential patterns of atypical asymmetry in autism.

To conclude, we report functional organization asymmetry in autism, its age-related changes, and trait relevance. In particular, we detected decreased leftward asymmetry in the language network along the sensory-default gradient and somatomotor network along the default-multiple demand gradient in autism. A differing developmental trajectory in autism was observed in the language network along the default mode-multiple demand gradient. Moreover, functional asymmetry is a central feature of autism, linking to autistic traits, with marked deviations from controls in terms of development and idiosyncrasy. Future work may study the impact of environmental factors upon genes associated with autism during early development and associated traits and cognitive development across the lifespan.

METHODS

We employed five datasets that covered children, adolescents, and young adults from the Autism Brain Imaging Data Exchange (ABIDE, https://fcon_1000.projects.nitrc.org/indi/abide), of which ABIDE-I includes New York University Langone Medical Center (NYU-I), University of Pittsburgh-School of Medicine (Pitt), and University of Utah-School of Medicine (USM), and ABIDE-II includes NYU-II and Trinity Center for Health Sciences-Trinity College Dublin (TCD). In accordance with HIPAA guidelines and 1000 Functional Connectomes Project / INDI protocols, all ABIDE datasets have been anonymized, with no protected health information included.

Participants

We restricted our analyses to males ($n = 300$) due to the low number of females with autism, consistent with previous work [4]. Individuals with autism underwent a structured or unstructured in-person interview and had

a diagnosis of Autistic, Asperger's, or Pervasive Developmental Disorder Not-Otherwise-Specified. These were established by expert clinical opinion aided by 'gold standard' diagnostics: Autism Diagnostic Observation Schedule Generic version (ADOS-G [85], and/or Autism Diagnostic Interview-Revised (ADI-R). Subdomains include communication, social interaction, and restricted repetitive behaviors (RRB). Intelligence quotient (IQ) was measured by the Wechsler Abbreviated Scale of Intelligence including III, IV, and V versions [86].

We excluded subjects with age greater than 40 years ($n = 2$) to retain a centralized population age and full IQ below 70 ($n = 1$) to avoid developmental delay of intelligence. Regarding head motion, we measured mean framewise displacement (FD), derived from Jenkinson's relative root mean square algorithm [87]. We excluded individuals whose mean FD was greater than 0.3 mm ($n = 14$), consistent with the previous report [4]. The final sample size taken into analyses was $n = 283$. Among these, we categorized them into three age groups including 142 young adults (18–40 years, autism: $n = 66$), 97 adolescents (12–17 years, autism: $n = 51$), and 76 children (6–11 years, autism: $n = 40$).

To reduce the effects of data sites, we conducted data harmonization (Fortin et al., 2018) using the toolbox neuroCombat (https://github.com/Jfortin1/neuroCombat). It provides a Bayesian approach to balance the effects of each scanner/site as well as continuous or categorized covariates. FIQ and head motion were entered as covariates during data harmonization. Results remain consistent and can be seen in our online iPython notebook.

Preprocessing of resting state fMRI data

High-resolution T1-weighted images (T1w) and resting-state functional magnetic resonance imaging (fMRI) data were available from all five sites. The scanning parameters and preprocessing procedures are reported in previous work [4]. In short, 3D-TurboFLASH was used for T1w of NYU datasets and 3D-MPRAGE was used for T1w of the other three datasets. TR ranged from 2100 to 300 ms and TE from 2.91 to 3.90 ms. The resolution was 1.1*1.0*1.1 mm^3 voxels. A 2D EPI sequence was employed for resting state fMRI data with the TR ranging from 1500 to 2000 ms, volumes ranging from 180 to 236 (NYU-I: 176, PITT: 196, USM: 236, TCD: 210, NYU-II: 180), and a resolution of 3.0*3.0*3.4 mm^3 voxels.

T1w data processing was done with FreeSurfer (v5.1; http://surfer.nmr.mgh.harvard.edu/). Image processing included bias field correction, registration to stereotaxic space, intensity normalization, skull-stripping, and white matter segmentation. Our fMRI analysis was based on preprocessed data previously made available by the Preprocessed Connectomes initiative (http://preprocessed-connectomesproject.org/abide/). Preprocessing was based on C-PAC (https://fcp-indi.github.io/) and included slice-time correction, head motion correction, skull stripping, and intensity normalization. Statistical corrections removed effects of head motion, white matter, and cerebrospinal fluid signals using the CompCor tool, based on the top 5 principal components, as well as linear/quadratic trends. After band-pass filtering (0.01–0.1 Hz), we co-registered resting state fMRI and T1w data in MNI152 space through combined linear and non-linear transformations.

Surface alignment was verified for each case and we interpolated voxel-wise rs-fMRI time-series along the mid-thickness surface. We resampled rs-fMRI surface data to downsampled Conte69 (10 k vertices per hemisphere), a template mesh from the HCP pipeline (https://github.com/Washington-University/Pipelines), and applied surface-based smoothing (FWHM = 5 mm). MRI quality control was complemented by assessment of signal-to-noise ratio and visual scoring of surface extractions for T1w.

Parcellation

To reduce the high computational demands of processing vertex-based fMRI data, we downsampled vertex-based fMRI data to 180 parcels per hemisphere using multimodal parcellation (MMP [57], and summarized features into Cole-Anticevic (CA) 12 functional networks [58]. MMP has been generated using the gradient-based parcellation approach with similar gradient ridges presenting in roughly corresponding locations in both hemispheres, which is suitable for studying asymmetry across homologous regions. Regarding cortical functional communities, CA atlas summarizes 12 functional networks based on MMP including primary visual (Vis1), secondary visual (Vis2), somatosensory (SMN), cingulate-opercular (CON), dorsal attention (DAN), language (Lan.), frontoparietal (FPN), auditory (Aud.), default mode (DMN), posterior-multimodal (PMN), ventral-multimodal (VMN), and orbito-affective (OAN).

Functional connectome gradients

After parcellating the preprocessed time series, we obtain the arrays of time series * parcels. We first computed the Pearson correlation between parcels using time series and transformed r values to z values using Fisher z-transformation. This generates the functional connectivity (FC) matrices of 360*360 for each individual. Then, to compute the functional connectome gradients, we used a non-linear manifold learning algorithm, to perform dimensionality reduction of the FC matrix. Consistent with the framework of asymmetry of functional gradients [31], we aligned each individual gradient to the template gradient (i.e., left-left group level gradients) with Procrustes rotation to make individual gradients comparable [30]. To gain an unbiased left-left group-level gradients template, without age or gender bias, in young adults, we employed data from Human Functional Connectome project S1200 release (HCP S1200). This has been done previously [31]. Briefly, we averaged 1104 subjects FC matrices of HCP S1200 and computed the group level gradients based on the mean left-left FC matrix. The first eigenvectors reflect unimodal-transmodal gradient (G1), sensory-visual gradient (G2), and multi-demand gradient (G3) explaining 24.1, 18.4, and 15.1% of total variance each.

Gradient analysis was performed in BrainSpace [30], a Matlab/python toolbox for brain dimensionality reduction (https://brainspace.readthedocs.io/en/latest/pages/install.html). Gradients are low dimensional eigenvectors of the connectome, along which cortical nodes that are strongly interconnected, by either many suprathreshold edges or few very strong edges, are situated closer together. Similarly, nodes with little connectivity are farther apart. This reflects the similarity/dissimilarity of functional connectivity profiles, which can be interpreted as functional integration and segregation between regions described in the form of a common coordinate space [33] built by the first three gradients. The name of this approach, which belongs to the family of graph Laplacians, is derived from the equivalence of the Euclidean distance between points in the diffusion map embedding [32, 88]. It is controlled by a single parameter α, which reflects the influence of the density of sampling points on the manifold ($\alpha = 0$, maximal influence; $\alpha = 1$, no influence). On the basis of the previous work [32], we followed recommendations and set $\alpha = 0.5$, a choice that retains the global relations between data points in the embedded space and has been suggested to be relatively robust to noise in the covariance matrix. The top 10% of values in the FC matrix were used for the threshold to enter the computation, consistent with previous studies [4, 31, 32].

Asymmetry index

To quantify the left and right hemisphere differences, we chose left-right as the asymmetry index (AI) [31]. We did not opt for normalized AI, i.e., (left-right)/(left +right), as gradient variance (normalized angle) has both negative and positive values [14] and normalized AI exaggerates the difference values or results in a discontinuity in the denominator [89]. The normalized AI is highly similar to non-normalized AI with correlation coefficients greater than 0.9 [31]. For the intra-hemispheric pattern, the AI was calculated using left-to-left connectome gradients minus right-to-right connectome gradients. A positive AI-score meant that the hemispheric feature dominated leftwards, while a negative AI-score dominated rightwards. For the inter-hemispheric pattern, we used left-to-right connectome gradients minus right-to-left connectome gradients to calculate the AI. We added a 'minus' to Cohen's d scores in the figures in order to conveniently view the lateralization direction (i.e., leftward or rightward).

Heritability and meta-analytic decoding

Regarding the meta-analytic decoding, we used functional MRI activation data from the NeuroSynth database [59]. We selected 24 cognitive domain terms, consistent with previous studies [31, 32, 38, 90]. In the present study, to decode both hemispheres, we separately fed the t values for the left and right hemisphere to the NeuroSynth. Then we generated 20 bins for the brain map (5% per bin) according to the t values. For each cognitive domain term, we averaged the activation z-score within each bin. To assess what functional processes may link to the regions observed to differ between controls and individuals with autism, we studied the association between the t values of the group difference map and meta-analytical maps. We calculated a weighted score by mean activation (where activation z-score greater than 0) multiplied by loading of the t values per bin. A bigger shape in the word cloud reflects a higher weighted score (i.e., atypically lateralized intrinsic functional organization in autism).

The heritability data were derived from a prior study by our team [31] that was based on a study of non-autistic adult twins/non-twins. After selecting the parcels where autism showed differences from NAI, we could describe their genetic underpinnings with heritability data from HCP.

Prediction

We performed supervised machine learning to predict the ADOS total and subscale scores. Regarding cross-validation, we applied a 5-fold leave-one-out strategy to learn the data. Among the 5-time iterations, the one with averaged MAE was chosen as the final model to predict the clinical symptoms. Linear regression with elastic net (L1_ratio = 0.1) was used as the feature selector. This follows an Empirical Bayesian approach to balance the effects of each scanner/batch. After the features' contributions had been built, we used Pearson correlation coefficients to evaluate how strong the model could be applied to the current sample.

First, we divided the participants into training and testing samples using a 4 to 1 ratio. Next, we applied data harmonization for training and testing samples separately. We then used the cross-validation as described above to select features in the training sample. The selected features were then fit in the independent testing sample to evaluate the model. We permuted the whole procedure 100 times with a random number to split the participants into training and testing samples. This enabled us to know the frequency of how often features are selected over the 100 permutations.

Data and code availability

The ABIDE open data can be acquired from https://fcon_1000.projects.nitrc.org/indi/abide/. All the analysis scripts and visualization for this study are openly available at a Github repository (https://github.com/wanbpsych/autism_gradient_asymm). Key dependencies are Python 3.9 (https://www.python.org/), BrainSpace (https://brainspace.readthedocs.io/), and BrainStat (https://brainstat.readthedocs.io/).

REFERENCES

1. Xu G, Strathearn L, Liu B, Bao W. Prevalence of autism spectrum disorder among US children and adolescents, 2014-2016. JAMA. 2018;319:81–2.
2. American Psychiatric Association. Diagnostic and statistical manual of mental disorders (5th ed.) [Internet]. Available from: https://dsm.psychiatryonline.org/doi/book/10.1176/appi.books.9780890425596.
3. Chen L, Chen Y, Zheng H, Zhang B, Wang F, Fang J, et al. Changes in the topological organization of the default mode network in autism spectrum disorder. Brain Imaging Behav. 2021;15:1058–67.
4. Hong SJ, Vos de Wael R, Bethlehem RAI, Lariviere S, Paquola C, Valk SL, et al. Atypical functional connectome hierarchy in autism. Nat Commun. 2019;10:1022.
5. Jung M, Kosaka H, Saito DN, Ishitobi M, Morita T, Inohara K, et al. Default mode network in young male adults with autism spectrum disorder: relationship with autism spectrum traits. Mol Autism. 2014;5:35.
6. Nunes AS, Peatfield N, Vakorin V, Doesburg SM. Idiosyncratic organization of cortical networks in autism spectrum disorder. NeuroImage. 2019;190:182–90.
7. Oldehinkel M, Mennes M, Marquand A, Charman T, Tillmann J, Ecker C, et al. Altered connectivity between cerebellum, visual, and sensory-motor networks in autism spectrum disorder: results from the EU-AIMS Longitudinal European Autism Project. Biol Psychiatry Cognit Neurosci Neuroimaging. 2019;4:260–70.
8. Ornitz EM. The modulation of sensory input and motor output in autistic children. J Autism Child Schizophr. 1974;4:197–215.
9. Park BY, Hong SJ, Valk SL, Paquola C, Benkarim O, Bethlehem RAI, et al. Differences in subcortico-cortical interactions identified from connectome and microcircuit models in autism. Nat Commun. 2021;12:2225.
10. Park S, Haak KV, Cho HB, Valk SL, Bethlehem RAI, Milham MP, et al. Atypical integration of sensory-to-transmodal functional systems mediates symptom severity in autism. Front Psychiatry. 2021;12:699813.
11. Valk SL, Di Martino A, Milham MP, Bernhardt BC. Multicenter mapping of structural network alterations in autism. Hum Brain Mapp. 2015;36:2364–73.
12. Washington SD, Gordon EM, Brar J, Warburton S, Sawyer AT, Wolfe A, et al. Dysmaturation of the default mode network in autism. Hum Brain Mapp. 2014;35:1284–96.
13. Postema MC, van Rooij D, Anagnostou E, Arango C, Auzias G, Behrmann M, et al. Altered structural brain asymmetry in autism spectrum disorder in a study of 54 datasets. Nat Commun. 2019;10:4958.
14. Sha Z, van Rooij D, Anagnostou E, Arango C, Auzias G, Behrmann M, et al. Subtly altered topological asymmetry of brain structural covariance networks in autism spectrum disorder across 43 datasets from the ENIGMA consortium. Mol Psychiatry. 2022;27:2114–25.
15. Floris DL, Wolfers T, Zabihi M, Holz NE, Zwiers MP, Charman T, et al. Atypical brain asymmetry in autism—a candidate for clinically meaningful stratification. Biol Psychiatry Cognit Neurosci Neuroimaging. 2021;6:802–12.
16. Floris DL, Howells H. Atypical structural and functional motor networks in autism. In: Forrester GS, Hopkins WD, Hudry K, Lindell A, editors. Progress in Brain Research [Internet]. Elsevier; 2018. p. 207–48. (Cerebral Lateralization and Cognition: Evolutionary and Developmental Investigations of Behavioral Biases; 238). Available from: https://www.sciencedirect.com/science/article/pii/S0079612318300554.
17. Jouravlev O, Kell AJE, Mineroff Z, Haskins AJ, Ayyash D, Kanwisher N, et al. Reduced language lateralization in autism and the broader autism phenotype as assessed with robust individual-subjects analyses. Autism Res. 2020;13:1746–61.
18. Just MA, Cherkassky VL, Keller TA, Minshew NJ. Cortical activation and synchronization during sentence comprehension in high-functioning autism: evidence of underconnectivity. Brain. 2004;127:1811–21.
19. Lindell AK, Hudry K. Atypicalities in cortical structure, handedness, and functional lateralization for language in autism spectrum disorders. Neuropsychol Rev. 2013;23:257–70.
20. Nielsen JA, Zielinski BA, Fletcher PT, Alexander AL, Lange N, Bigler ED, et al. Abnormal lateralization of functional connectivity between language and default mode regions in autism. Mol Autism. 2014;5:8.
21. Hartwigsen G, Bengio Y, Bzdok D. How does hemispheric specialization contribute to human-defining cognition? Neuron. 2021;109:2075–90.
22. Gotts SJ, Jo HJ, Wallace GL, Saad ZS, Cox RW, Martin A. Two distinct forms of functional lateralization in the human brain. Proc Natl Acad Sci. 2013;110:E3435–44.
23. Benkarim O, Paquola C, Park BY, Hong SJ, Royer J, Vos de Wael R, et al. Connectivity alterations in autism reflect functional idiosyncrasy.Commun Biol. 2021;4:1–15.
24. Hahamy A, Behrmann M, Malach R. The idiosyncratic brain: distortion of spontaneous connectivity patterns in autism spectrum disorder. Nat Neurosci. 2015;18:302–9.
25. Floris DL, Barber AD, Nebel MB, Martinelli M, Lai MC, Crocetti D, et al. Atypical lateralization of motor circuit functional connectivity in children with autism is associated with motor deficits. Mol Autism. 2016;7:35.
26. Cardinale RC, Shih P, Fishman I, Ford LM, Müller RA. Pervasive rightward asymmetry shifts of functional networks in autism spectrum disorder. JAMA Psychiatry. 2013;70:975–82.
27. Kleinhans NM, Müller RA, Cohen DN, Courchesne E. Atypical functional lateralization of language in autism spectrum disorders. Brain Res. 2008;1221:115–25.
28. Flagg EJ, Cardy JEO, Roberts W, Roberts TPL. Language lateralization development in children with autism: Insights from the late field magnetoencephalogram. Neurosci Lett. 2005;386:82–7.
29. Hong SJ, Xu T, Nikolaidis A, Smallwood J, Margulies DS, Bernhardt B, et al. Toward a connectivity gradient-based framework for reproducible biomarker discovery. NeuroImage. 2020;223:117322.
30. Vos de Wael R, Benkarim O, Paquola C, Lariviere S, Royer J, Tavakol S, et al. BrainSpace: a toolbox for the analysis of macroscale gradients in neuroimaging and connectomics datasets. Commun Biol. 2020;3:1–10.
31. Wan B, Bayrak Ş, Ting Xu T, Schaare HL, Bethlehem RA, Bernhardt BC, et al. Heritability and cross-species comparisons of human cortical functional organization asymmetry. Elife. 2022;11:e77215.
32. Margulies DS, Ghosh SS, Goulas A, Falkiewicz M, Huntenburg JM, Langs G, et al. Situating the default-mode network along a principal gradient of macroscale cortical organization. Proc Natl Acad Sci. 2016;113:12574–9.
33. Huntenburg JM, Bazin PL, Margulies DS. Large-scale gradients in human cortical organization. Trends Cognit Sci. 2018;22:21–31.
34. Paquola C, Amunts K, Evans A, Smallwood J, Bernhardt B. Closing the mechanistic gap: the value of microarchitecture in understanding cognitive networks. Trends Cognit Sci. 2022;26:873–86.
35. Smallwood J, Bernhardt BC, Leech R, Bzdok D, Jefferies E, Margulies DS. The default mode network in cognition: a topographical perspective. Nat Rev Neurosci. 2021;22:503–13.
36. Bernhardt BC, Smallwood J, Keilholz S, Margulies DS. Gradients in brain organization. NeuroImage. 2022;251:118987.
37. Dong HM, Margulies DS, Zuo XN, Holmes AJ. Shifting gradients of macroscale cortical organization mark the transition from childhood to adolescence. Proc Natl Acad Sci. 2021;118. Available from: https://www.pnas.org/content/118/28/e2024448118.
38. Valk SL, Xu T, Paquola C, Park BY, Bethlehem RAI, Vos de Wael R, et al. Genetic and phylogenetic uncoupling of structure and function in human transmodal cortex. Nat Commun. 2022;13:2341.
39. Xia Y, Xia M, Liu J, Liao X, Lei T, Liang X, et al. Development of functional connectome gradients during childhood and adolescence. Sci Bull. 2022; Available from: https://www.sciencedirect.com/science/article/pii/S2095927322000020.
40. Gonzalez Alam TR del J, Mckeown BLA, Gao Z, Bernhardt B, Vos de Wael R, et al. A tale of two gradients: differences between the left and right hemispheres predict

semantic cognition. Brain Struct Funct. [Internet]. 2021; Available from: https://doi.org/10.1007/s00429-021-02374-w.
41. Liang X, Zhao C, Jin X, Jiang Y, Yang L, Chen Y, et al. Sex-related human brain asymmetry in hemispheric functional gradients. NeuroImage. 2021;229:117761.
42. Boucher J. Research review: structural language in autistic spectrum disorder – characteristics and causes. J Child Psychol Psychiatry. 2012;53:219–33.
43. Hong SJ, Mottron L, Park BY, Benkarim O, Valk SL, Paquola C, et al. A convergent structure–function substrate of cognitive imbalances in autism. Cereb Cortex. 2023;33:1566–80.
44. Kjellmer L, Fernell E, Gillberg C, Norrelgen F. Speech and language profiles in 4- to 6-year-old children with early diagnosis of autism spectrum disorder without intellectual disability. Neuropsychiatr Dis Treat. 2018;14:2415–27.
45. Vogindroukas I, Stankova M, Chelas EN, Proedrou A. Language and speech characteristics in autism. Neuropsychiatr Dis Treat. 2022;18:2367–77.
46. Demetriou EA, Lampit A, Quintana DS, Naismith SL, Song YJC, Pye JE, et al. Autism spectrum disorders: a meta-analysis of executive function. Mol Psychiatry. 2018;23:1198–204.
47. Zhang Z, Peng P, Zhang D. Executive function in high-functioning autism spectrum disorder: a meta-analysis of fMRI studies. J Autism Dev Disord. 2020;50:4022–38.
48. Kong XZ, Mathias SR, Guadalupe T, Group ELW, Glahn DC, Franke B, et al. Mapping cortical brain asymmetry in 17,141 healthy individuals worldwide via the ENIGMA Consortium. Proc Natl Acad Sci. 2018;115:E5154–63.
49. Roe JM, Vidal-Piñeiro D, Sørensen Ø, Brandmaier AM, Düzel S, Gonzalez HA, et al. Asymmetric thinning of the cerebral cortex across the adult lifespan is accelerated in Alzheimer's disease. Nat Commun. 2021;12:721.
50. Bethlehem RAI, Paquola C, Seidlitz J, Ronan L, Bernhardt B, Consortium CC, et al. Dispersion of functional gradients across the adult lifespan. NeuroImage. 2020;222:117299.
51. Colvert E, Tick B, McEwen F, Stewart C, Curran SR, Woodhouse E, et al. Heritability of autism spectrum disorder in a UK population-based twin sample. JAMA Psychiatry. 2015;72:415–23.
52. Tick B, Bolton P, Happé F, Rutter M, Rijsdijk F. Heritability of autism spectrum disorders: a meta-analysis of twin studies. J Child Psychol Psychiatry. 2016;57:585–95.
53. Di Martino A, Yan CG, Li Q, Denio E, Castellanos FX, Alaerts K, et al. The autism brain imaging data exchange: towards large-scale evaluation of the intrinsic brain architecture in autism. Mol Psychiatry. 2014;19:659–67.
54. Di Martino A, O'Connor D, Chen B, Alaerts K, Anderson JS, Assaf M, et al. Enhancing studies of the connectome in autism using the autism brain imaging data exchange II. Sci Data. 2017;4:170010.
55. Fortin JP, Cullen N, Sheline YI, Taylor WD, Aselcioglu I, Cook PA, et al. Harmonization of cortical thickness measurements across scanners and sites. NeuroImage. 2018;167:104–20.
56. Larivière S, Bayrak Ş, Vos de Wael R, Benkarim O, Herholz P, Rodriguez-Cruces R, et al. BrainStat: a toolbox for brain-wide statistics and multimodal feature associations. NeuroImage. 2023;266:119807.
57. Glasser MF, Coalson TS, Robinson EC, Hacker CD, Harwell J, Yacoub E, et al. A multi-modal parcellation of human cerebral cortex. Nature. 2016;536:171–8.
58. Ji JL, Spronk M, Kulkarni K, Repovš G, Anticevic A, Cole MW. Mapping the human brain's cortical-subcortical functional network organization. NeuroImage. 2019;185:35–57.
59. Yarkoni T, Poldrack RA, Nichols TE, Van Essen DC, Wager TD. Large-scale automated synthesis of human functional neuroimaging data. Nat Methods. 2011;8:665–70.
60. Paquola C, Benkarim O, DeKraker J, Larivière S, Frässle S, Royer J, et al. Convergence of cortical types and functional motifs in the human mesiotemporal lobe. ELife. 2020;9:e60673.
61. Park BY, Park H, Morys F, Kim M, Byeon K, Lee H, et al. Inter-individual body mass variations relate to fractionated functional brain hierarchies. Commun Biol. 2021;4:1–12.
62. Turnbull A, Karapanagiotidis T, Wang HT, Bernhardt BC, Leech R, Margulies D, et al. Reductions in task positive neural systems occur with the passage of time and are associated with changes in ongoing thought. Sci Rep. 2020;10:9912.
63. Floris DL, Chura LR, Holt RJ, Suckling J, Bullmore ET, Baron-Cohen S, et al. Psychological correlates of handedness and corpus callosum asymmetry in autism: the left hemisphere dysfunction theory revisited. J Autism Dev Disord. 2013;43:1758–72.
64. Knaus TA, Silver AM, Lindgren KA, Hadjikhani N, Tager-Flusberg H. fMRI activation during a language task in adolescents with ASD. J Int Neuropsychol Soc. 2008;14:967–79.
65. Solomon-Harris LM. Atypical lateralization of language and face processing in autism spectrum disorder. 2022; Available from: https://yorkspace.library.yorku.ca/xmlui/handle/10315/39586.
66. Williams LZJ, Fitzgibbon SP, Bozek J, Winkler AM, Dimitrova R, Poppe T, et al. Structural and functional asymmetry of the neonatal cerebral cortex. Nat Hum Behav. 2023;7:942–55.
67. Luyster R, Lopez K, Lord C. Characterizing communicative development in children referred for Autism Spectrum Disorders using the MacArthur-Bates Communicative Development Inventory (CDI)*. J Child Lang. 2007;34:623–54.
68. Szaflarski JP, Holland SK, Schmithorst VJ, Byars AW. fMRI study of language lateralization in children and adults. Hum Brain Mapp. 2006;27:202–12.
69. Guadalupe T, Mathias SR, vanErp TGM, Whelan CD, Zwiers MP, Abe Y, et al. Human subcortical brain asymmetries in 15,847 people worldwide reveal effects of age and sex. Brain Imaging Behav. 2017;11:1497–514.
70. Zhou D, Lebel C, Evans A, Beaulieu C. Cortical thickness asymmetry from childhood to older adulthood. NeuroImage. 2013;83:66–74.
71. Di Martino A, Fair DA, Kelly C, Satterthwaite TD, Castellanos FX, Thomason ME, et al. Unraveling the miswired connectome: a developmental perspective. Neuron. 2014;83:1335–53.
72. Geschwind DH, Miller BL, DeCarli C, Carmelli D. Heritability of lobar brain volumes in twins supports genetic models of cerebral laterality and handedness. Proc Natl Acad Sci. 2002;99:3176–81.
73. Sha Z, Schijven D, Carrion-Castillo A, Joliot M, Mazoyer B, Fisher SE, et al. The genetic architecture of structural left–right asymmetry of the human brain. Nat Hum Behav. 2021;5:1226–39.
74. Gazzaniga MS. Cerebral specialization and interhemispheric communication: does the corpus callosum enable the human condition? Brain. 2000;123:1293–326.
75. Toga AW, Thompson PM. Mapping brain asymmetry. Nat Rev Neurosci. 2003;4:37–48.
76. Anderson JS, Druzgal TJ, Froehlich A, DuBray MB, Lange N, Alexander AL, et al. Decreased interhemispheric functional connectivity in autism. Cereb Cortex. 2011;21:1134–46.
77. Freitag CM, Luders E, Hulst HE, Narr KL, Thompson PM, Toga AW, et al. Total brain volume and corpus callosum size in Medication-Naïve Adolescents and young adults with autism spectrum disorder. Biol Psychiatry. 2009;66:316–9.
78. Paul LK, Corsello C, Kennedy DP, Adolphs R. Agenesis of the corpus callosum and autism: a comprehensive comparison. Brain. 2014;137:1813–29.
79. McGlone J. Sex differences in functional brain asymmetry. Cortex. 1978;14:122–8.
80. McGlone J. Sex differences in human brain asymmetry: a critical survey. Behav Brain Sci. 1980;3:215–27.
81. Floris DL, Peng H, Warrier V, Lombardo MV, Pretzsch CM, Moreau C, et al. The link between autism and sex-related neuroanatomy, and associated cognition and gene expression. Am J Psychiatry. 2023;180:50–64.
82. Fombonne E. The prevalence of autism. JAMA 2003;289:87–9.
83. Hull L, Mandy W, Petrides K. Behavioural and cognitive sex/gender differences in autism spectrum condition and typically developing males and females. Autism. 2017;21:706–27.
84. Lai MC, Lombardo MV, Auyeung B, Chakrabarti B, Baron-Cohen S. Sex/gender differences and autism: setting the scene for future research. J Am Acad Child Adolesc Psychiatry. 2015;54:11–24.
85. Lord C, Risi S, Lambrecht L, Cook EH, Leventhal BL, DiLavore PC, et al. The autism diagnostic observation schedule—generic: a standard measure of social and communication deficits associated with the spectrum of autism. J Autism Dev Disord. 2000;30:205–23.
86. Wechsler D. Wechsler abbreviated scale of intelligence (WASI). San Antonio, TX: Psychological Corporation; 1999.
87. Jenkinson M, Bannister P, Brady M, Smith S. Improved optimization for the robust and accurate linear registration and motion correction of brain images. NeuroImage. 2002;17:825–41.
88. Coifman RR, Lafon S. Diffusion maps. Appl Comput Harmon Anal. 2006;21:5–30.
89. Nielsen JA, Zielinski BA, Ferguson MA, Lainhart JE, Anderson JS. An evaluation of the left-brain vs. right-brain hypothesis with resting state functional connectivity magnetic resonance imaging. PLOS One. 2013;8:e71275.
90. Wang Y, Royer J, Park BY, Vos de Wael R, Larivière S, Tavakol S, et al. Long-range functional connections mirror and link microarchitectural and cognitive hierarchies in the human brain. Cereb Cortex. 2022;33:1782–98.

ACKNOWLEDGEMENTS

We are grateful to the open access platform for neuroimaging data sharing in autism: ABIDE (https://fcon_1000.projects.nitrc.org/indi/abide/). BCB. acknowledges research support from the National Science and Engineering Research Council of Canada (NSERC Discovery-1304413), Canadian Institutes of Health Research (FDN-154298, PJT-174995), SickKids Foundation (NI17-039), BrainCanada, FRQ-S, and the Tier-2 Canada Research Chairs program. SLV and BCB are furthermore funded by the Helmholtz International BigBrain Analytics and Learning Laboratory (HIBALL), supported by the Helmholtz Association's Initiative and Networking Fund and the Healthy Brains, Healthy Lives initiative at McGill University. SLV is supported by the Otto Hahn Award at Max Planck Society, and BW is supported by the International Max Planck Research School on Neuroscience of Communication: Function, Structure, and Plasticity (IMPRS NeuroCom) and Graduate Academy Leipzig.

AUTHOR CONTRIBUTIONS

BW: Conceptualization, Methodology, Formal analysis, Writing - Original Draft, Writing - Review & Editing, Visualization, Project administration, Funding acquisition. S-JH: Methodology, Data Curation, Writing - Review & Editing. RAI Bethlehem: Writing - Review & Editing. DLF: Writing - Review & Editing. BCB: Writing - Review & Editing, Funding acquisition. SLV: Conceptualization, Methodology, Writing - Original Draft, Writing - Review & Editing, Supervision, Funding acquisition.

FUNDING

Open Access funding enabled and organized by Projekt DEAL.

COMPETING INTERESTS

The authors declare no competing interest.

ADDITIONAL INFORMATION

Supplementary information The online version contains supplementary material available at https://doi.org/10.1038/s41380-023-02220-x.

Correspondence and requests for materials should be addressed to Bin Wan or Sofie L. Valk.